arXiv:1806.08310v1 [hep-ph] 21 Jun 2018

Probing compressed dark sectors at 100 TeV in the dileptonic mono-Z channel

Rakhi Mahbubani[a] **and José Zurita**[b,c]

[a]*Institut de Théorie des Phenomènes Physiques, EPFL, Lausanne, Switzerland*

[b]*Institute for Nuclear Physics (IKP), Karlsruhe Institute of Technology, Hermann-von-Helmholtz-Platz 1, D-76344 Eggenstein-Leopoldshafen, Germany*

[c]*Institute for Theoretical Particle Physics (TTP), Karlsruhe Institute of Technology, Engesserstraße 7, D-76128 Karlsruhe, Germany*

E-mail: rakhi@cern.ch, jose.zurita@kit.edu

ABSTRACT: We examine the sensitivity at a future 100 TeV proton-proton collider to compressed dark sectors whose decay products are invisible due to below-threshold energies and/or small couplings to the Standard Model. This scenario could be relevant to models of WIMP dark matter, where the lightest New Physics state is an (isolated) electroweak multiplet whose lowest component is stable on cosmological timescales. We rely on the additional emission of a hard on-shell Z-boson decaying to leptons, a channel with low background systematics, and include a careful estimate of the real and fake backgrounds to this process in our analysis. We show that an integrated luminosity of 30 ab^{-1} would allow exclusion of a TeV-scale compressed dark sector with inclusive production cross section of 0.3 fb, for 1% background systematic uncertainty and splittings below 5 GeV. This translates to exclusion of a pure higgsino (wino) multiplet with mass of 500 (970) GeV.

1 Introduction

The current state of particle physics brings to mind the (apparently apocryphal [1]) Chinese curse "May you live in interesting times". That the complete absence of any evidence for Physics Beyond the Standard Model (BSM) at the LHC is interesting is undeniable. What is less clear is how to interpret it: does it signal a need for a paradigm shift in our understanding of naturalness of the electroweak scale, or is New Physics simply better concealed than we had expected?

The latter could occur if the lowest-lying new states are near-degenerate in mass, leading to decay products that are below detection thresholds, particularly if the lightest state in this compressed spectrum is collider-stable and interacts weakly with ordinary matter, making it invisible to our detectors. Production of these compressed states at hadron colliders are thus indistinguishable from uninteresting Standard Model (SM) background, unless the missing energy is enhanced by recoil of the invisible system against a hard visible SM state X which can then be used for triggering and analysis.

Such 'dark sectors' may be independently motivated by thermal relic dark matter, as TeV-scale electroweak multiplets with a thermal history have a density consistent with the measured relic abundance [2].[1]

The prevailing wisdom from mono-X searches is that the hadronic channels (monojet, and hadronic mono-W and mono-Z) give the strongest constraints on pair-production of invisible states, followed by the monophoton channel, with a far reduced sensitivity acheivable in leptonic mono-Z. As pointed out in [4] this trend is not simply due to the relative production rate for each channel, since the cross section for the corresponding irreducible background scales similarly (see Fig. 1). Hence, for a search whose background is sufficiently small that its uncertainty is statistics-dominated, one would naively expect the ratio of significances monojet : monophoton : mono-Z to scale like $1 : q\sqrt{\alpha/\alpha_s} : \sqrt{\mathrm{BR}(Z)\alpha_Z/\alpha_s}$ for $\alpha_i = g_i^2/4\pi$ and $\mathrm{BR}(Z)$ the branching ratio of the channel the visible Z boson decays to.[2] By this measure the dileptonic mono-Z channel is approximately a fiftieth as sensitive to compressed dark states as the monojet, and around a tenth as sensitive as the monophoton.

Omitted in this argument is the effect of systematics, which is undoubtedly large due to the large backgrounds. Moreover, as the leading (subleading) background in the monojet (mono-Z) channel scale as the gluon Parton Distribution Function (PDF), we would expect the background systematics to grow with energy. In the regime where the background uncertainty is dominated by systematic effects there is now an inherent *disadvantage* to using the monojet channel, since the sensitivity scales like $S/(\beta B)$, for sytematics factor β, and the coupling ratios cancel.

Of course this comparison is rather simplistic and a number of additional effects must be taken into account before drawing a conclusion: the kinematic suppression due to the production of the Z boson at LHC energies, as compared with the logarithmic enhancement of the monojet and monophoton rates, for instance. This last effect would be partially mitigated at a high-energy hadron collider like the FCC-hh. For $\sqrt{s} \gg m_Z$, the Z-boson

---

[1]This would require a large tuning in the mass of the Higgs, however we find naturalness considerations misplaced as a motivation for a future circular collider, touted as a machine of the 'post-naturalness era' [3].

[2]Here we assumed that the relative efficiencies for the signal and background processes are similar across the different mono-X channels. This is not unlikely for a total background dominated by the SM irreducible component, with an on-shell Z decaying invisibly.

Mono-jet   Mono-photon   Mono-Z (dileptonic)

Signal

Background

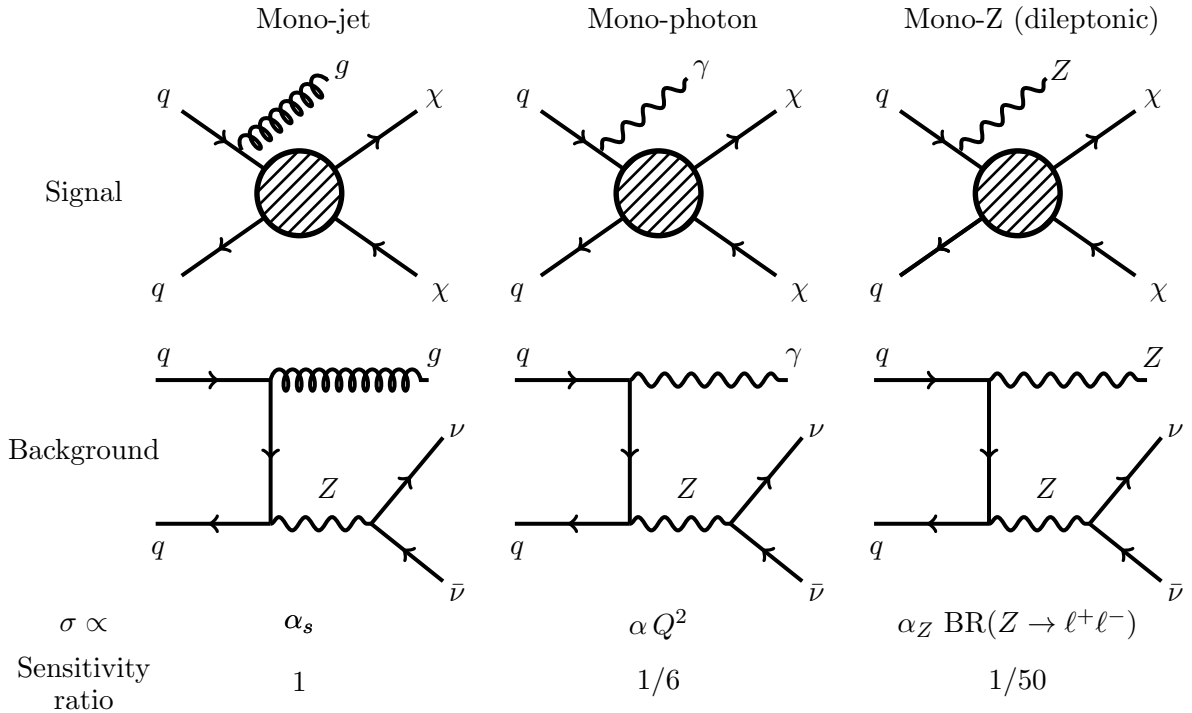| $\sigma \propto$	α_s	$\alpha\,Q^2$	$\alpha_Z\,\mathrm{BR}(Z\to\ell^+\ell^-)$
Sensitivity ratio	1	1/6	1/50

Figure 1: Relative signal sensitivity in the three main mono-X channels. Since the cross sections for each signal and its irreducible background scale in the same way, if we assume the relative effiency for the signal and background processes are the same over each of the different channels, the naive sensitivity, computed as $S/\sqrt{B}$, scales as $\sqrt{\alpha_S} : Q\sqrt{\alpha} : \sqrt{\alpha_Z\mathrm{BR}(Z\to\ell^+\ell^-)}$. However this argument does not account for systematic uncertainties, which we expect will grow at higher centre-of-mass energy.

can be thought of as effectively massless, allowing us to neglect the additional phase space suppression from production of a massive state, and giving rise to sudakov divergences which would also need resummation, as for jet and photon emission. Moreover the strong coupling runs down at high energies, giving the monojet channel less of an advantage due to coupling alone, We believe these factors warrant a reassessment of the reach for compressed states in the leptonic mono-Z channel, as compared with that in the monojet channel [5], at FCC energies.

Existing limits on the reach for compressed dark sectors can be found in [6–11]. The reach at hadron colliders has been covered in various studies: e.g [12–16] consider monojet searches; [17–19] look at the monophoton channel [19–22] look at leptonic mono-Z. Other searches rely on the detection of soft daughter particles from decays within the compressed sector [5, 14, 15], although their sensitivity is strongly dependent on p_T reconstruction thresholds, which will necessarily increase at a future collider. The reach due to disappearing charged tracks from a highly-boosted charged component can be found in [5, 18, 23]. There are in addition cosmological constraints on pure electroweakino relics, although the prospects for discovery of a wino-like relic are rather more promising [24, 25]. Nearly pure higgsino-like multiplets instead remain elusive [26], although recent studies speculate on the possibility of probing this scenario using observations of compact stars [27] or neutron

stars [28].

In this work, we explore the reach at the FCC-hh for compressed dark-sector states in the dileptonic mono-Z channel, making careful consideration of both real and fake Standard Model backgrounds. Our results are given both as contours of production cross section required for exclusion at a given mass and splitting, for ease of recasting, as well as a reach for a pure higgsino-like dark sector, which is a simple and compelling example of a thermal relic. The cross section limits would hold in many scenarios with production of a long-lived neutral state, such as some models of neutrino mass [29–31], or ones containing Higgs portals with tiny couplings [32, 33].

Our paper is organized as follows. Section 2 contains specifics of our analysis, with the simplified model used for simulation purposes detailed in Section 2.1. Event generation, backgrounds and cuts, including an extended discussion of shapes of missing transverse energy (MET) distributions is contained in Section 2.2. Our results, including some discussion of the effect of higher-order corrections are shown in Section 3; and we interpret these in the context of a pure higgsino thermal relic in Section 4, which will also be constrained by future indirect- and direct-detection experiments. We conclude in Section 5.

2 Mono-Z analysis

2.1 Simplified model

For the purposes of simulation and analysis, we focus on the case with a dark sector consisting of a weak doublet $\chi = (\chi^+, \chi^0)$, with hypercharge $Y = -1/2$ and Dirac mass m_χ. We include tree-level mixing effects with a heavy electroweak-singlet fermion with Majorana mass m_S, as shown in Eq.(2.1)

$$\mathcal{L} \supset i\bar{\chi}\,\slashed{D}\chi + \frac{i}{2}\bar{\lambda}\,\slashed{\partial}\lambda - m_\chi\bar{\chi}\chi - \frac{m_S}{2}\bar{\lambda}\lambda - y_L\bar{\lambda}H^\dagger P_L\chi + y_R\bar{\lambda}HP_R\chi + \text{h.c.} \qquad (2.1)$$

We take all parameters to be real[3] and fix the yukawa couplings to the corresponding values in the neutralino sector of the Minimal Supersymmetric Standard Model (MSSM) for concreteness, with $\tan(\beta) = 15$. We focus on the experimentally-challenging regime of large m_S, which corresponds to the MSSM in the pure higgsino limit. In this regime the heaviest neutral state χ_3^0, which is almost pure singlet, is irrelevant for the collider phenomenology, and can be ignored. Moreover, after electroweak symmetry breaking the mass mixing with the singlet splits the neutral Dirac fermion into two Majorana fermions χ_1^0 and χ_2^0; for large m_S the mass splitting between these two states, $\Delta_0 = \chi_2^0 - \chi_1^0$ is too small to give rise to detectable decay products:

$$\Delta_0 \sim 200\,\text{MeV}\left(\frac{10\,\text{TeV}}{m_S}\right). \qquad (2.2)$$

This is also the case for the charged-neutral splitting $\Delta_+ = m_{\chi^+} - m_{\chi^0}$, which gets an additional contribution from electroweak loops of $\Delta_{\text{1-loop}} \sim \mathcal{O}(\alpha\,m_Z) \sim 300\,\text{MeV}$ [35].

Rather than the Lagrangian input parameters, we will will express our results in terms of the phenomenologically-relevant parameter set (m_χ, Δ_+), using the latter as a proxy for the average mass splitting within the dark sector. Our search sensitivity will be strongly

---

[3]Although the system contains one irreducible phase [34] this has no effect on the collider phenomenology.
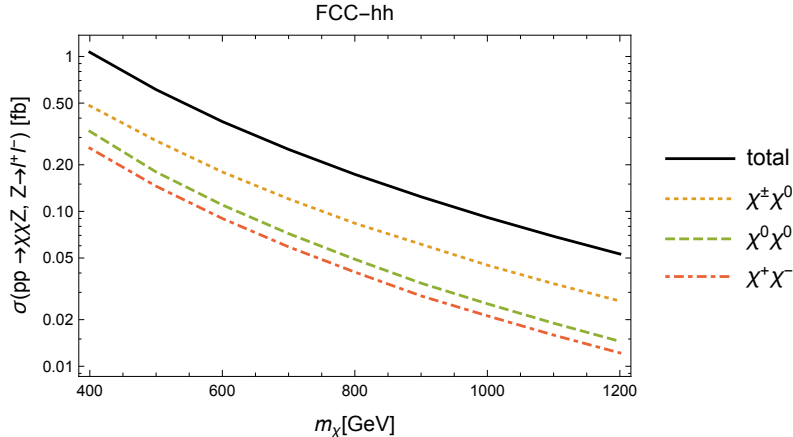
Figure 2: Inclusive production cross sections for $pp \rightarrow \chi\chi Z$, $(Z \rightarrow \ell^+\ell^-)$, for weak-doublet Dirac fermion χ with hypercharge -1/2 at a future hadron-hadron collider with 100 TeV centre-of-mass energy. We assume that inter-state splittings are small enough to have a negligible effect.

dependent on m_χ, which fixes the production cross section for a given electroweak representation (in the small-mixing limit), and also determines the kinematics of the events. By contrast the sensitivity has a weak dependence on Δ_+, through the cut efficiencies, and only for Δ_+ above a certain threshold, beyond which the visible decay products have enough energy to fall foul of our object vetos.[4] Below this threshold, which we see is around 5 GeV, ours is a one-parameter analysis which is completely insensitive to the details of the decays. As such we can apply the limits on the total production cross section obtained in this scenario as a conservative estimate on the sensitivity in this channel to arbitrary compressed dark sectors, produced in association with a leptonically-decaying Z, provided the dark sector can be approximately characterized by a single mass scale.

If the lightest neutral component of the multiplet, χ_1^0, is stable on cosmological timescales, it becomes a good candidate for dark matter, saturating the relic density at a mass of 1.1 TeV [2, 36]. For a relic χ, the presence of a tree-level splitting Δ_0 due to mixing with the heavy singlet is essential for it not to be ruled out by direct detection experiments, a vector-like coupling between dark matter and the SM Z-boson being long-excluded due to too large a scattering cross section with ordinary matter.

We show in Fig. 2 the inclusive production cross section for pair-production of a weak-doublet χ with hypercharge -1/2, in association with a leptonically-decaying $Z-$ boson, for negligible inter-state splittings. This ranges from 1 fb for a mass of 400 GeV to 0.05 fb at 1.2 TeV.

2.2 Event generation

We manually implemented the simplified model above via the *usr_mod* feature in `MadGraph5 v2.3.3` [37], and tested it against existing MSSM implementations. Widths and branching fractions were computed using analytic expressions given in Appendix A of [23] (and references therein), and input manually, since existing SUSY spectrum generators do not

---

[4]In this regime the contribution to the splitting due to electroweak loop effects are sub-dominant.

cover the regime where tree-level mixing is small and the masses of the SM fermion decay products are relevant.

Our signal consists of the production of a pair of electroweakinos recoiling against a hard leptonically-decaying Z-boson, giving rise to two leptons plus missing transverse energy in the final state. We simulate leading-order $\chi\bar{\chi}Z$ production, and the leptonic decay of the Z boson, in `MadGraph5 v2.3.3` with the CTEQ6L1 parton distributions [38], and allow `Pythia v6.4` [39] to handle dark sector decays, parton showering and hadronization. We use `Delphes v.3.2.0` [40] for detector simulation, with an FCC-hh card that is customized to impose no detector-level lepton isolation in order to maximize our sensitivity to highly-boosted Z-bosons. We instead impose a naive analysis-level isolation-based rejection of leptons that are within $\Delta R < 0.2$ of a jet. (See object selection below.) Jets are clustered with FASTJET's [41] anti-kt algorithm [42] for a jet radius of R=0.4. Events were read using `MadAnalysis5` [43, 44] and analysed using in-house code.

Backgrounds, which were also simulated using the above pipeline, can be split into three categories:

- real backgrounds: Processes giving rise to two leptons and missing energy at parton level. This includes the diboson processes $ZZ \to l^+l^-\nu\nu$ and $W^+W^- \to l^+\nu l^-\nu$, as well as fully-leptonic $t\bar{t}$. These are simulated at leading order.

- one fake/lost lepton: Processes that have less than (more than) two hard leptons at parton level, requiring the mis-identification of jets as leptons (one or more leptons to be missed). These include semi-leptonic $t\bar{t}$ (merged and matched up to one additional jet), (leptonic) W + jets (merged and matched up to two jets) and fully-leptonic WZ (simulated at parton level).

- fake MET: The missing energy in these processes arises mainly from mis-measurement of the transverse momenta of hard jets. This category includes $Z \to l^+l^-$ + jets (matched up to two jets), and also the diboson processes ZZ and ZW, with one Z decaying leptonically and the other gauge boson decaying hadronically (simulated at parton level).

- fake leptons and fake MET: The leading contribution to this category of background events would come from QCD multijets, which has a huge cross section. In principle we would expect an increased contribution from multijets to the total background at the FCC-hh as compared with the LHC, since this process grows with the square of the gluon PDF. It is however difficult to estimate its contribution due to generation efficiencies, and we assume this will be negligible after our selection cuts, as it is in existing mono-Z analyses at the LHC.

Generator-level cuts are imposed on the missing energy (and proxies thereof) in order to improve the efficiency of both signal and background generation. For any process with a real leptonically-decaying Z-boson and E_T^{miss}, we impose a hard cut on the transverse momentum of the Z, $p_T(Z) > 400$ GeV. For all other backgrounds with real E_T^{miss}, we impose $E_T^{\mathrm{miss}} > 400$ GeV at parton level, while backgrounds with fake E_T^{miss} have a hard cut on $H_T = \sum_{\mathrm{jets}} |p_T| > 400$ GeV as a proxy for the maximum E_T^{miss} in the process. The value chosen for this cut is sufficiently below our initial selection so as not to affect the final cross section.

Our object selection is as follows:

- $p_T > 100$ (60) GeV for jets (leptons);

- for leptons: $\Delta_R(l, j) < 0.2$. We exclude any leptons that do not satisfy this criterion.

We pre-select events with:

- exactly two opposite sign, same flavour leptons, which reconstruct an on-shell Z, $M_{l^+l^-} \in [76, 106]$ GeV;

- $p_T(Z) > 450$ GeV;

- $\Delta\phi(j_{1,2}, E_T^{\mathrm{miss}}) \geq 0.2$ to reduce jets faking E_T^{miss};

Our events consist of three independent elements that recoil against each other in the transverse plane: a reconstructed Z, E_T^{miss}, and one or more additional jets, with total transverse momentum $\sum_{\mathrm{jets}} \vec{p}_T$. The relative proportions of these three components vary
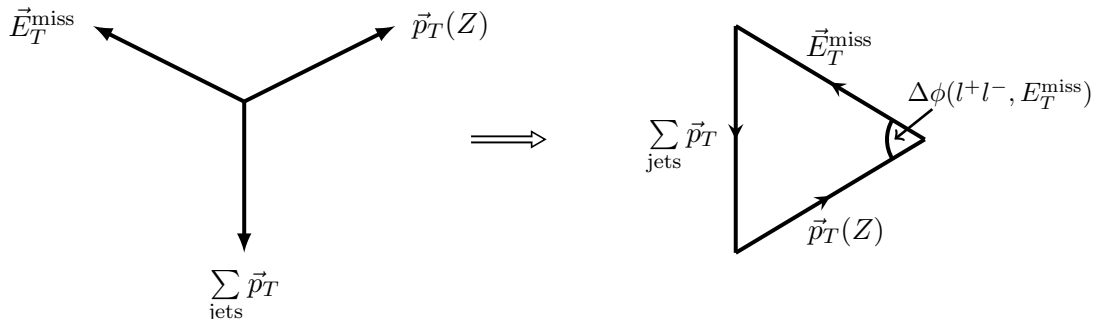

Figure 3: Sketch of different components of $Z + E_T^{\mathrm{miss}}$ events in the transverse plane: the dilepton system recoils against the missing energy and the vector sum of hadronic p_T. Conservation of transverse momentum implies the vectors form a closed triangle, which can be defined by the lengths of two sides and the enclosed angle, or by the lengths of all three sides.

between the signal and backgrounds processes, with conservation of transverse momentum requiring that the three vectors form a closed triangle, see Fig. 3. Hence the transverse kinematics of any event are completely fixed by specifying the lengths of the three sides of the triangle, or equivalently the lengths of two sides and the enclosed angle. Signal events will mostly resemble an isosceles triangle, with a hard Z recoiling against missing energy, and some additional soft hadronic activity. Backgrounds with fake MET, on the other hand, will tend more towards equilateral in shape.

For universality across different dark sector mass scales, we re-express these three dimensionful quantities as two dimensionless ratios, $p_T(Z)/E_T^{\mathrm{miss}}$ and H_T/E_T^{miss}, for $H_T = \sum_{\mathrm{jets}} |\vec{p}_T|$, with the magnitude of the missing energy setting the overall mass scale. We gain in sensitivity by using the scalar sum, H_T, rather than the vector sum of jet transverse momenta (or equivalently $\Delta\phi(Z, E_T^{\mathrm{miss}})$), since the former is also sensitive to back-to-back jets, and hence is a better measure of total hadronic activity. Moreover, H_T and E_T^{miss} share some systematics related to jet-mismeasurement, which would cancel to a large extent in the ratio. Note that we use H_T as computed by Delphes using reconstruction-level jets, which is unaffected by our hard jet selection above.
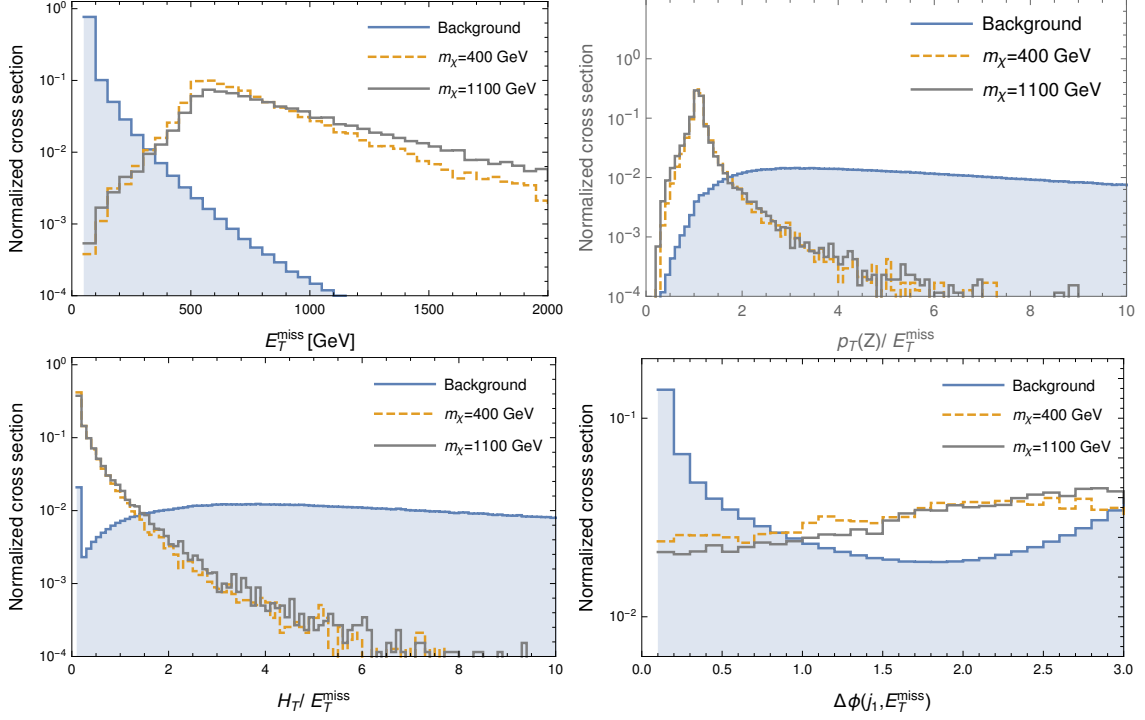
Figure 4: Unit-normalized kinematic distributions after preselection for signal points with masses 1.1 TeV (solid) and 400 GeV (dashed), and nominal charged-neutral splitting, and the sum of the three leading backgrounds (shaded) (Z+jets, $ZZ \to l^+l^-jj$ and $WZ \to \ell^+\ell^-\ell\nu$).

Cuts on variables outside the transverse plane, such as lepton pseudorapidities [21], or angular variables in the rest frame of the Z [45] are ineffective here, since the production mechanisms of the signal and irreducible background are identical.

In Fig. 4 below we display normalized distributions of relevant kinematic variables after preselection cuts, for dominant backgrounds and two signal parameter points: $m_\chi = 400, 1100$ GeV with negligible splitting. The latter point saturates the thermal relic density measurement (see Section 4 for details). We see that there is significant separation between signal and background shape in the variables, with the different signal distributions looking rather similar over the entire mass range of interest.

Based on these distributions we add to the preselection a preliminary soft E_T^{miss} cut

- $E_T^{\text{miss}} \geq 450$ GeV,

and optimize the signal sensitivity (defined as $S/\sqrt{B}$) with respect to the dimensionless kinematic variables shown. We find that the sensitivity is maximized by imposing the following additional cuts on signal and backgrounds:

- $x \equiv p_T(Z)/E_T^{\text{miss}} < 1.3$;

- a hard cut on hadronic activity, $y \equiv H_T/E_T^{\text{miss}} < 1.4$.

Optimizing individually for each parameter point yields efficiency differences that are below 0.1%. We further impose a floating E_T^{miss} cut that is optimized for each m_χ.

Process	Preselection	$x < 1.3$	$y < 1.4$	$E_T^{\mathrm{miss}} > 550$ GeV	$E_T^{\mathrm{miss}} > 900$ GeV
Signal A	176	168	163		72
Signal B	1234	1184	1166	914	
$ZZ \to l^+l^-\nu\nu$	83799	81292	81178	51623	11172
$W^+W^- \to l^+\nu l^-\nu$	< 1	< 1	< 1	< 1	< 1
$tt \to l^+b\nu l^-\bar{b}\nu$	5136	4484	3980	2300	238
$tt \to l\nu b\bar{b}jj$	57161	44459	5835	3922	635
$(Z \to l^+l^-)$ +jets	321204	208220	48719	25174	4373
$(W \to l\nu)$+jets	2142	1797	72	66	24
$ZW \to l^+l^-l\nu$	11835	10891	10873	5935	889
$ZZ \to l^+l^-jj$	2021	819	339	137	13
$ZW \to l^+l^-jj$	301	113	36	15	3
10^3 S$_A$/B	0.36	0.48	1.08		4.14
Significance A ($\beta = 0$)	0.25	0.28	0.42		0.55
Significance A ($\beta = 0.01$)	0.04	0.05	0.10		0.33
10^3 S$_B$/B	2.55	3.36	7.72	10.26	
Significance B ($\beta = 0$)	1.77	1.99	3.00	3.06	
Significance B ($\beta = 0.01$)	0.25	0.33	0.75	0.97	

Table 1: Cut flow for the backgrounds and for signal points with with masses 1.1 TeV (A) and 400 GeV (B), and nominal charged-neutral splitting (optimized for zero background systematics in each case). The numbers of events quoted correspond to a total integrated luminosity of 30 ab^{-1} at a 100 TeV center-of-mass energy. The significance is computed assuming a) no systematic errors and b) 1 % systematic errors.

3   Results

We display the cutflow for signal points with $m_\chi = 1.1$ TeV (Signal A) and $m_\chi = 400$ GeV (Signal B) with nominal splittings, and all relevant backgrounds in Table 1. The optimal missing energy cut for benchmark A (B), in the absence of systematic uncertanties, is $E_T^{\mathrm{miss}} > 900$ (550) GeV. We include signal-to-background ratios, S/B and significances, both with and without systematic uncertainties, without re-optimizing. The significance including systematics is computed as $S/\sqrt{(B + \beta^2 B^2)}$ for $\beta =$1%.

We see from Table 1 that while Z+jets is the dominant source of background before optimization, after all cuts its proportion decreases to around 30% of the total, with the irreducible di-Z process accounting for most of the remainder. Sub-dominant backgrounds include $ZW \to \ell^+\ell^-\ell\nu$ and top quark production in the semileptonic and pure leptonic channels. The background composition is consistent with that in the 13 TeV, 2.3 fb^{-1} CMS study [46].[5] Neglecting the Z+jets background would lead to an increase of 15-20% in significance for our signal points. Note that these sensitivities are contingent upon our ability to successfully reconstruct the Z using highly-boosted leptons. The detrimental effect on the significance of a lower limit on the lepton separation that can be resolved is shown in appendix A.

Clearly the main issue in this analysis is the huge irreducible di-Z background, whose distributions closely mirror those of the signal. Conventional wisdom holds that a hard enough cut in missing energy can help suppress this background to reasonable levels, the signal having a larger fraction of events at high MET. This is not the case here, where the larger available centre-of-mass energy means we can access energy scales that are much

---

[5]The most recent analyses by CMS [9] and ATLAS [47] have the proportion of Z+jets decreasing to around 5% of the total background due to a hard cut in $\Delta\phi(Z, E_T^{\mathrm{miss}})$. However this is a result we are unable to achieve in our 100 TeV analysis without cutting away our signal entirely, as the proportion of V+jets in the background increases with the gluon PDF.
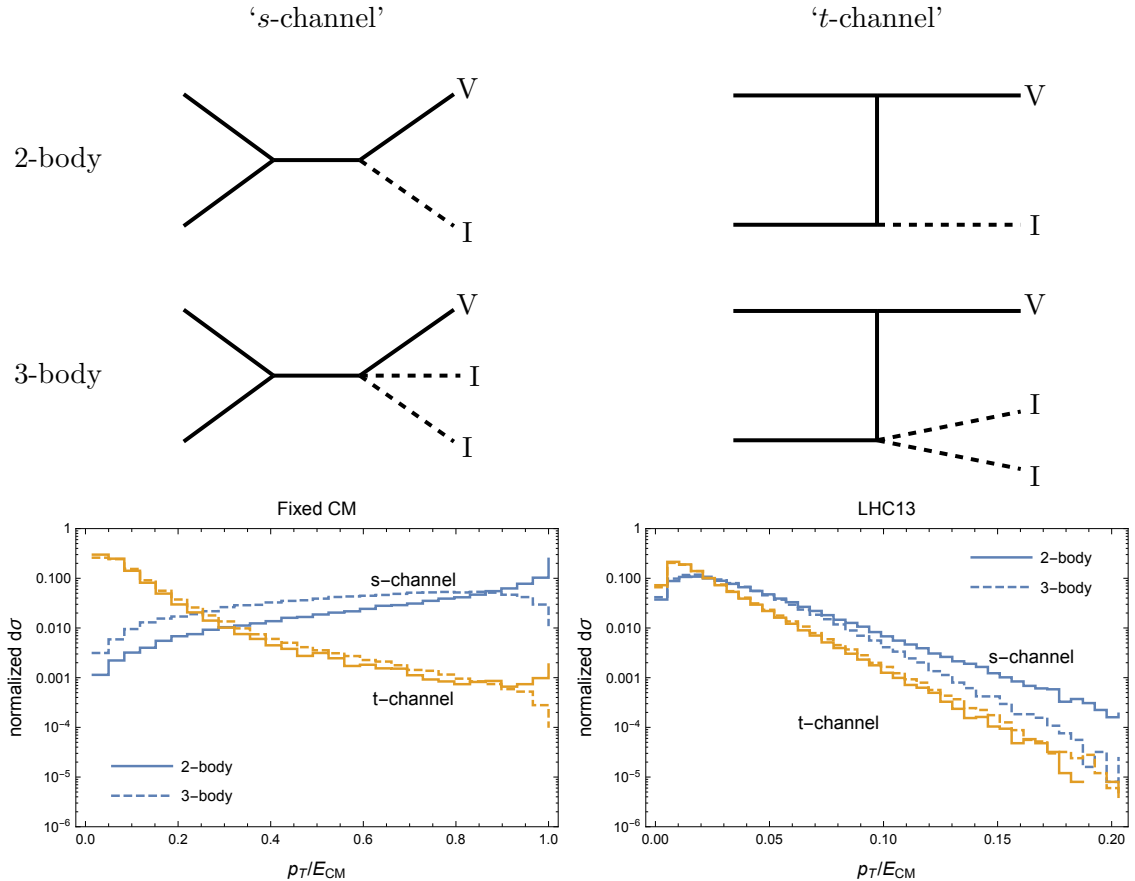
Figure 5: Normalized MET distributions for 's-channel' and 't-channel', 2- and 3-body topologies, with visible final state V and invisible states I. The 2-body t-channel topology corresponds to the irreducible SM di-Z background, as well as $\chi\bar{\chi}Z$ production via an on-shell mediator. A compressed dark state produced instead via an off-shell gauge boson mediator, as it is here, is a 3-body, t-channel process.

larger than any relevant mass scale. Any difference in the shape of the MET spectra of the signal and irreducible background is limited to the region below the dark sector mass scale; far above this scale both the Z-boson and dark sector particles are effectively massless, hence cutting at arbitrarily high E_T^{miss} does not enhance the signal sensitivity. We can gain some further understanding of the power of the MET spectrum by considering the phase space and production topologies for the signal and irreducible background in MET+X processes.

Interlude: MET shapes

First, consider the MET spectrum from pure phase space considerations (which is also the spectrum for production processes with an s-channel propagator). At fixed center-of-mass energy the MET distribution for a two-body semi-visible final state has a jacobian peak at its endpoint, familiar from the transverse mass distribution of the W boson. The visible p_T distribution is instead significantly softened for a three-body process with one visible final-state particle, since we must integrate over a larger number of un-measured

(invisible) momenta [48]. A similar pattern must also be evident, although less obvious, at a hadron collider, where the pure phase space distributions are convoluted with a falling PDF. Although there is now no jacobian peak, the MET spectrum for the two-body process is still harder than that for the three-body one. This effect is illustrated in Fig. 5, where the distributions were generated using Madgraph simulations of a simplified model with multiple scalars. If our signal and irreducible background were produced via this s-channel topology, the latter would have a harder MET spectrum, since it is a two-body process, and cutting on MET would be counterproductive.

Instead both the three-body signal process $\chi\bar{\chi}Z$ and the two-body background ZZ are produced in the 't-channel', defined in the right-hand panel of Fig. 5.[6] Production via a t-channel propagator favours forward emission, as pointed out in [49]. This can mask the phase space effect, resulting in two- and three-body p_T spectra that are much more similar in shape (and softer than the s-channel case) both at fixed and variable centre-of-mass energies. This argument also holds for the mono-W, monophoton and mono-higgs channel. In the monojet case it is further complicated by the fact that the final state gluon can also be crossed into the initial state, giving a final MET spectrum that is some combination of t- and s-channel production.

This also means that any MET+X search will be maximally sensitive to a dark sector where $\chi\bar{\chi}X$ can be produced dominantly from an s-channel process via an on-shell dark mediator. It would be a fun exercise to find a viable model in which this occurs, and recast current MET+X limits in the context of such a topology.

Binned MET exclusion

Even though the irreducible background could in principle be estimated precisely using measurements of related di-boson processes, as in [50], even small systematic effects can completely swamp our signal, especially at low masses where backgrounds are large, leaving no exclusion in the mass range of interest. It is particularly beneficial in such a situation to move to a binned analysis, where we can benefit maximally from shape differences between the MET distribution for the signal and total background (see Fig. 4, first panel). This minimizes the effect of background systematics, which in the case where the uncertainties are uncorrelated in different bins, would dominantly affect the background normalization rather than its shape, and is the method of choice in the most recent $E_T^{\mathrm{miss}} + X$ searches at the LHC (see e.g. [7]).

We use the profile likelihood method to compute the 95% CLs exclusion on the total inclusive $\chi\chi + Z$, $(Z \to \ell^+\ell^-)$ cross section, σ^{95}. We bin both signal and background using 200-GeV E_T^{miss} bins, after preselection and x and y cuts, which largely eliminate the fake background, and our results are independent of the binning for reasonable bin widths. Details of our method are deferred to Appendix B.

We plot in Fig. 6 (left panel) the median expected exclusion (continuous blue line) as well as the 1σ bands (shaded region) as a function of χ mass, for negligible splitting and a background systematic uncertainty of 1%, at the FCC-hh with an integrated luminosity of 30 ab^{-1}. The LO cross section for a pure higgsino with nominal splitting is shown as a dashed blue line, from which we see that the reach in this channel corresponds to a pure higgsino mass of around 500 GeV. We also show in the right-hand panel of Fig. 6

---

[6]Note that in the three-body topologies an offshell particle connecting the s- and t-channel propagators to the two invisible states has been omitted for simplicity, since its presence has no impact on the MET shape.

contours of σ^{95} in the two-dimensional plane (m_χ, Δ_+), with the contour width reflecting the difference in the result for 1% and 2% systematic uncertainties. Note that the limit is rather insensitive to the splitting for small splittings, but gets weaker for large splittings, as decay products become hard enough to be visible, and events are vetoed. The sensitivity in the latter region could be improved by allowing for additional soft leptons

As mentioned above, our analysis cuts are based purely on the kinematics of t-channel production, rather than details of the spin or couplings. Hence we expect they can be used as a conservative limit on many scenarios featuring pair-produced dark sector particles of mass m_χ and small splitting Δ_+, although specific features of other scenarios could of course be exploited to yield tighter constraints.
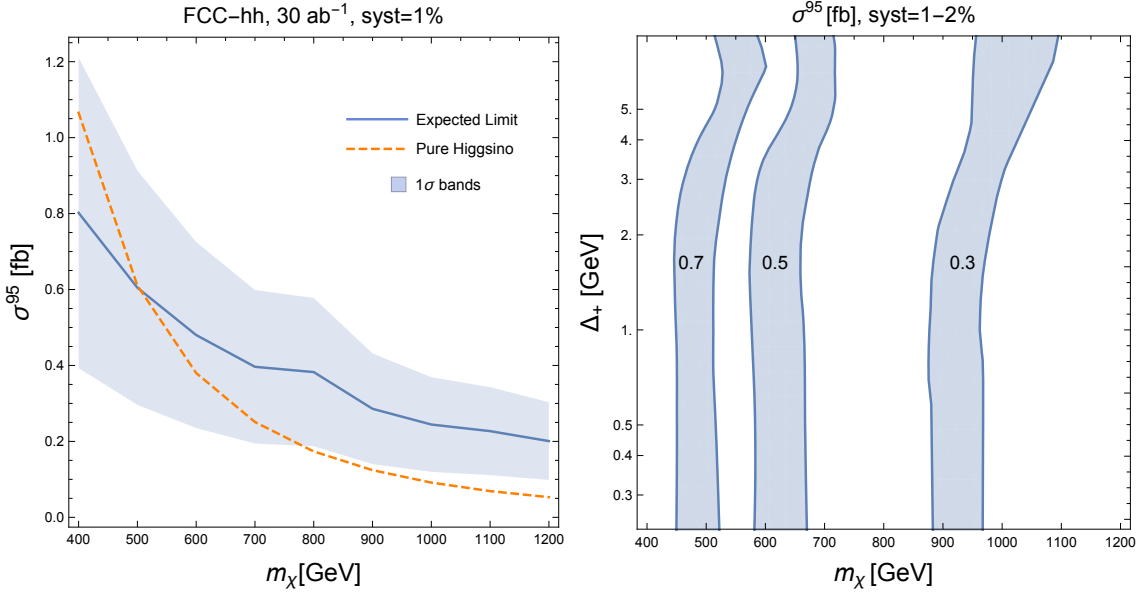

Figure 6: (Left panel) Median expected limit on the inclusive cross section $\bar{\chi}\chi + (Z \to \ell^+\ell^-)$ at 95% CLs, σ^{95} (continuous blue line) and 1σ bands (shaded region), as a function of dark sector mass, for negligible splitting and a background systematic uncertainty of 1%. The expected cross section for a pure higgsino with nominal splitting is shown for comparison (dashed line). (Right panel) Contours of σ^{95} as a function of dark sector mass and splitting, for background systematic uncertainties of 1-2%. Results were computed for a weak doublet with hypercharge -1/2 and nominal splitting, at FCC-hh, for a total integrated luminosity of 30 ab^{-1}.

Higher-order corrections

Sources of sub-leading corrections to our process of interest, and the results given above include:

- Next-to-leading order (NLO) QCD corrections. This effect can be parameterized by a multiplicative K-factor, K_{QCD}, that we expect is approximately equal for the signal and the irreducible background. It can yield a 20-30% boost in the ZZ cross section at LHC13 [49, 51], although we expect the effect to be relatively smaller at higher scales due to the running of the strong gauge coupling.

- Electroweak sudakov suppression due to large logarithms $\mathcal{O}\left(\log p_T/m_{Z,W}\right)$ [52]. These arise because initial (and typically, final) states are not $SU(2)$ singlets, so logarithms do not completely cancel between real and virtual correction, and generically give rise to a large suppression of the leading order cross section, which increases for increasing Z-boson p_T. We estimate that the suppression to the diboson background is approximately the square of the suppression in the signal, leading to no effect on the significance, to first approximation.

- The effect due to the running of the $SU(2)$ coupling is negligible.

Assuming the background is dominated by the irreducible component, the effect of higher order corrections would be an enhancement in the overall significance by a factor $\sqrt{K_{\mathrm{QCD}}}$, or equivalently, a reduction in the excluded cross section by the same factor.

4 Pure higgsino thermal relic

We will now place these results in a more specific context, that of a thermal relic in the pure higgsino limit of the MSSM, with an abundance today that depends on its mass and splittings, the latter being fixed by mixing with the bino. We will consider current and future constraints from direct detection and additional collider searches that can have sensitivity to the parameter space of interest. Indirect detection is not presently sensitive to thermal relic higgsinos in this mass range [27, 53], and the large systematic uncertainties in the background make it difficult to make precise projections on future sensitivity. Hence we will neglect it in the following discussion.

In the limit of small splitting the thermal relic density is fixed by the gauge couplings of the higgsino [36]:

$$\Omega h^2 = 0.105 \left(\frac{\mu}{1\ \mathrm{TeV}}\right)^2. \tag{4.1}$$

Consistency with the current PLANCK measurement of $\Omega h^2 = 0.1198 \pm 0.0026$ [54] yields an upper limit on the doublet mass m_χ of [1.05-1.08] TeV.

For larger splittings we implemented the Lagrangian in Eq. (2.1) in `FeynRules v2.3` [55] using the interface to `CalcHEP v3.6.27` [56] in order to employ `micrOMEGAs v4.1.2` [57] for the calculation of dark matter properties. The regime of higgsino mass and splitting for which the relic density that would overclose the universe is shown as a grey shaded region in Fig. 7.

The higgsino parameter space is also constrained by the null results from direction detection experiments. In the limit $m_\chi \gg m_S$ (or equivalently $\mu \gg M_1 \gg M_2$ in the MSSM), the relevant interactions are proportional to the tree-level splittings.

$$L \supset \frac{g}{2c_W}\frac{\Delta_+ - \Delta_{\text{1-loop}}}{m_Z}\, h\, \bar{\chi}_1^0\chi_1^0 \;+\; \frac{g}{8c_w}\frac{\Delta_0}{m_\chi}\, \bar{\chi}_1^0 \slashed{Z}\gamma^5\chi_1^0\,, \tag{4.2}$$

We see from Eq. (4.2) that the coupling for Z-boson exchange, which results in a spin-dependent coupling to matter, is parametrically suppressed, as compared with the higgs-exchange term, by one to two orders of magnitude for the range of relic mass relevant to this study. Moreover the spin structure functions in spin-dependent detection are small, and don't scale with detector size due to the difficulty in engineering coherent spin over macroscopic detector lengths. Both these effects result in a spin-dependent cross section that is below the required sensitivity for detection [53].
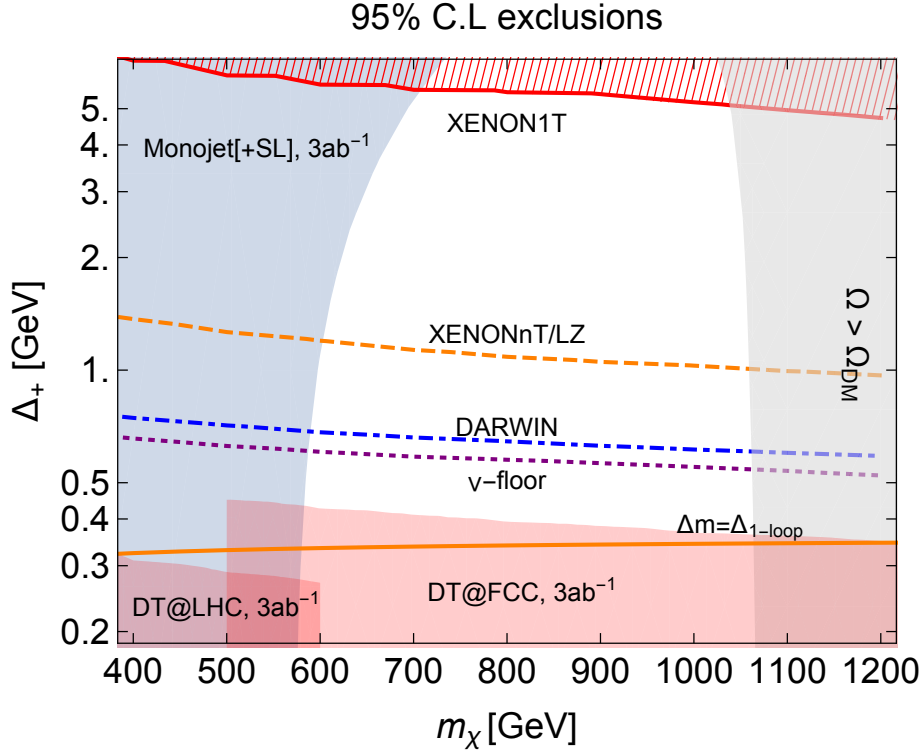
Figure 7: Status of the higgsino parameter space in view of current and future experimental constraints. We show the FCC monojet reach [5] (blue shaded) and the FCC disappearing track reach [23] (red shaded), for an integrated luminosity at FCC-hh of 3 ab^{-1}; as well as the region where the thermal relic overcloses the universe (grey shaded). The limit on the spin-independent direct-detection cross section due to the recent XENON1T results [58] is denoted by a red line, with the diagonal-filled region above the line excluded. The dashed and dash-dotted lines correspond to the sensitivity of future direct-detection experiments, with the splittings at which the neutrino floor becomes relevant shown in purple short dashes. The solid orange line corresponds to the nominal 1-loop electroweak splitting.

We focus instead on the spin-independent cross section with nucleons, which can be written [59]:

$$\sigma_{\text{SI/N}} = g_{h\chi\chi}^2 \frac{8G_F^2 m_Z^2 \sin^2\theta_W}{\pi} \left(\frac{m_N}{m_h}\right)^4 \left(\frac{1}{1 + \frac{m_N}{m_\chi}}\right)^2 \left(\frac{2}{9} + \frac{7(f_u^N + f_d^N + f_s^N)}{9}\right)^2 \quad (4.3)$$

for nucleon mass m_N and physical Higgs mass m_h, where $g_{h\chi\chi}$, in the small-mixing limit, is proportional to the tree-level charged-neutral splitting (see Eq. (4.3)). Following the recommendation of the LHC Dark Matter Working Group [60] we take equal proton and neutron masses, $m_N = 0.939$ GeV, and form factors: $f_u^N = 0.019$, $f_d^N = 0.045$ [61] and $f_s^N = 0.043$ [62], which gives:

$$\sigma_{\text{SI/N}} \approx (4 \times 10^{-47} \text{ cm}^2) \left(\frac{\Delta_+ - \Delta_{1-\text{loop}}}{\text{GeV}}\right)^2 \quad (4.4)$$

for $m_\chi \gg m_N$. Note that Eq. (4.4) is correct at first order in the small parameters m_Z/M_1, m_N/μ, and is only dependent on the additional MSSM input parameters $\tan\beta$ and $I = \mathrm{Sgn}(\mu)$ indirectly through the value of the tree-level splitting $(\Delta_+ - \Delta_{1-\mathrm{loop}})$ (as well as through terms that are higher order in m_Z/M_1). We can also see evidence of a 'blind spot' for direct detection [63], where the tree-level splitting goes to zero for $\tan\beta = 1$ and $I = -1$.

We show in Fig. 7 the region of the compressed higgsino parameter space that is consistent with the measured thermal relic density, along with the current exclusion based on the direct detection constraint recently announced by XENON1T [58]. We show also projected sensitivities for future experiments XENONnT/LZ [64, 65] and DARWIN [66]; and the neutrino floor [67], where new techniques will be required to reject significant backgrounds due to solar neutrinos. Our results are computed by numerically diagonalizing the neutralino mass matrix, and they agree at percent level with those computed at tree-level using microOMEGAS. Loop effects can be consistently included by running and matching the relevant operators over the different energy scales [68], this yields an additional contribution to the direct-detection cross section of $\sim 10^{-50}$ cm^2 in the pure higgsino limit, which is an order of magnitude below the level of the neutrino floor.

We add to Fig. 7 the collider constraints acheivable with 3 ab^{-1} of integrated luminosity at FCC-hh, using a monojet (+ soft lepton) search [5], and disappearing charged tracks with improved reconstruction of short charged tracks [23]. We see evidence in this figure of the true complementarity between the constraints on higgsino dark matter relic, and the collider constraints on the dark higgsino. The measurement of the relic abundance, and indirect detection and mono-X collider searches, probe the creation and annihilation of pairs of higgsinos, and are rather insensitive to the splittings (for small splittings), bounding the higgsino mass from left and right, respectively. By contrast, direct detection, which measures higgsino scattering, and disappearing charged track searches, which probes chargino decays, are crucially dependent on the splittings, and constrains these from above and below. The combined effect is a 'bracketing' of the available parameter space from all directions.

In Fig. 8 (left panel) we superimpose on this parameter space results from our binned mono-Z search with 30 ab^{-1} of integrated luminosity at FCC-hh and a background systematic uncertainty of 1% (solid black line) and 2% (dashed black line). We find that the mono-Z search can probe higgsinos of mass up to 500 (400) GeV, for splittings below 2 GeV, and a background systematic of 1% (2%). For these large backgrounds the reach is rather crucially dependent upon how well under control the background systematics are. Inclusion of a K-factor for NLO QCD correction, as per the naive procedure above, would push the limit up to 550 GeV. We can recast this as a limit on winos using the excluded cross section, and obtain a constraint on the wino mass of 970 GeV.

In the right panel of Fig. 8 we show the luminosity necessary for a 95% CLs exclusion on pure higgsinos, for 1% systematic uncertainty in the background. Combining 30 ab^{-1} of data from each of two experiments could push the limit above 600 GeV, but closing the pure higgsino window entirely would require over 600 ab^{-1} of integrated luminosity, making this goal rather unfeasible in the dileptonic mono-Z channel.

Figure 8: Higgsino parameter space covered by the existing studies and the proposed mono-Z search. (Left panel) The 95% CLs exclusion for our dileptonic mono-Z search, for 30 ab^{-1} of integrated luminosity at FCC-hh, and a background systematic uncertainty of 1% (solid black line) and 2% (dashed black line). Note that the other collider searches shown use a lower luminosity of 3 ab^{-1}. For more details see caption of Fig. 7 and text. (Right panel) Contours of luminosity required for 95% CLs exclusion, L^{95}, for 1% systematic uncertainty in the background.

5 Conclusions

In this work we made a careful assessment of the ultimate reach of a 100 TeV pp collider to compressed dark sectors, including some considerations of higher-order effects, in the dileptonic Z+MET channel. We arued that dismissing this channel in favour of the monojet on the basis of a cross-section argument alone is premature. The backgrounds to mono-X processes are large, making systematic effects important, and these, particularly for the monojet process, will likely be more significant in ther busier environment of a 100 TeV proton-proton machine.

The most promising handle we have on the signal is the MET distribution. The utility of this variable at the LHC is rooted in the fact that the pure phase-space behaviour, which would lead you to expect the two-body SM ZZ distribution to be harder than that of three-body BSM $\chi\chi Z$ process, is modified by the presence of a t-channel propagator in the production process, which favours forward Z emission, thus softening the MET spectrum. This effect is most severe in the 2-body case, and results in increasing signal significance for increasing MET cut, but only for MET values ranging from the Z mass to the new physics scale. Far above the mass of new physics, everything is effectively massless, and further cuts decrease the sensitivity.

Using a binned CLs method for the total signal and background MET distributions, we find a 95% exclusion on pure higgsinos of 500 GeV, with 30 ab^{-1} of integrated luminosity, for a rather optimistic estimate on the background systematic uncertainty of 1%. As with all mono-X searches, this reach is crucially dependent on the systematics, decreasing to 400 GeV if the systematic uncertainty is doubled. We find that NLO QCD effects raise the reach by 50 GeV, while electroweak sudakov factors have little effect, to first approximation, since their effect on the background will likely scale like the square of the

effect on the signal. This reach diminishes for intra-sector splittings of around 5 GeV; tagging soft decay products could yield additional sensitivity in this regime.

Such mono-X searches at future high-energy hadron colliders would work in concert with other collider searches, including the disappearing charged track search, as well as the astro-particle experimental programme, to bracket the available parameter space for compressed dark sectors. However future prospects for discovery of nearly-pure higgsino dark matter, still look bleak, particularly in the thermal regime. It is absurd to imagine that if nature really did work this way, we may still have no concrete evidence of it half a century from now! Although some ideas exist for teasing out the signature of a pure-higgsino relic from measurements of neutron stars and compact stars, their sensitivity remains unclear, as they are subject to large astrophysical uncertainties. What is clear, is that this situation is in urgent need of new ideas if we are to finally close the window on, or discover, electroweakino dark matter.

Acknowledgments

A   Lepton resolution

As stressed before, this study relies on our capability to reconstruct a Z from two highly-boosted leptons. The `Delphes` FCC card used when this project started had a $\Delta R(l^+, l^-)$ resolution of 0.03. The latest Delphes release further reduces this value to 0.013. It is thus a fair question to understand how the sensitivity degrades with the di-lepton resolution. Thus we present in Fig. 9 the significance as a function of $\Delta R_{\min}(l^+, l^-)$, where we impose the cut $\Delta R(l^+, l^-) > \Delta R_{\min}(l^+, l^-)$, for μ positive. In addition we superimpose there the $\Delta R_{\min} = (\Delta \eta^2 + \Delta \phi^2)^{1/2}$ obtained from the `Delphes` parameterization of the ATLAS, CMS and FCC detectors, where for simplicity we have taken the values corresponding to the central region of the calorimeters, namely $\Delta \phi = \pi/18, \pi/36, \pi/128, \pi/360$ and $\Delta \eta = 0.1, 0.087, 0.025, 0.01$ for ATLAS, CMS and the old and latest versions of the FCC respectively.

From the figure we see that even with the current specs for the FCC calorimeter the sensitivity does not degrade significantly, unlike what would happen if the LHC were going to be run with a 100 TeV center-of-mass energy. We thus conclude that resolving these highly-boosted leptons will not be a problem in the future, and we stress once again the importance of considering the detector design to maximize the impact of a future collider for the physics case under consideration.
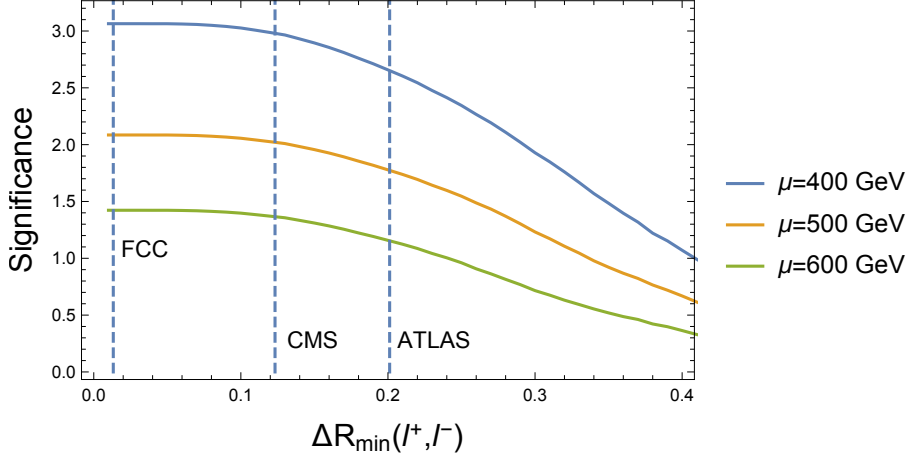
Figure 9: Significances as a function of the minimum resolvable distance between leptons, $\Delta R_{\min}(l^+, l^-)$ for a nominal $\Delta_+ = 344$ MeV. We have superimposed the $\Delta R_{\min}(l^+, l^-)$ values corresponding to the `Delphes` parameterizations of ATLAS, CMS and the FCC detectors.

B   Profile likelihood

We use the profile likelihood method to determine our sensitivity, with likelihood defined as follows:

$$L(\mu, \boldsymbol{\theta}) = \prod_{i=1}^{N} \frac{(\mu s_i + \theta_i)^{n_i}}{n_i} e^{-(\mu s_i + \theta_i)} \frac{1}{\sqrt{2\pi}\sigma_i} e^{-\frac{(b_i - \theta_i)^2}{2\sigma_i^2}} \tag{B.1}$$

where μ is the overall normalization of the signal, which has s_i events in each bin, and θ_i, a nuisance parameter that will be profiled over, is distributed as a gaussian with mean b_i (the expected number of background events in each bin) and variance σ_i given by the systematic uncertainty.

To find the expected exclusion we compute the usual test statistic using the Asimov dataset, $\sqrt{q_{\mu,A}}$ (see e.g. [69] for details). This is simple enough to do analytically, and yields:

$$q_{\mu,A} = \sum_i \left[-2b_i \log\left(\frac{\mu s_i + \hat{\theta}_A}{b_i}\right) - 2(b_i - \mu s_i - \hat{\theta}_A) - \frac{(b_i - \hat{\theta}_A)^2}{\sigma_i^2} \right] \tag{B.2}$$

for

$$\hat{\theta}_A = \frac{1}{2}\left[b_i - \mu s_i - \sigma_i^2 + \sqrt{\left(b_i + \mu s_i - \sigma_i^2\right) + 4b_i\sigma_i^2} \right] . \tag{B.3}$$

In the limit $s_i \ll b_i + \sigma_i^2$ this reduces to the sum over the familiar rule-of-thumb expression $s_i/\sqrt{b_i + \sigma_i^2}$ for each bin. The CLs p-value is given in the asymptotic limit by [69]:

$$p_{\mu,A} = \frac{p_s}{1 - p_b} = \frac{1 - \Phi(\sqrt{q_{\mu,A}})}{\Phi(0)} \tag{B.4}$$

and we can compute the exclusion at 95% confidence by numerically solving for the normalization factor μ^{95} that gives $p_{\mu,A} = 0.05$, at each signal mass m_χ.

References

[1] Wikipedia, "May you live in interesting times."

[2] M. Cirelli, N. Fornengo, and A. Strumia, *Minimal dark matter*, *Nucl. Phys.* **B753** (2006) 178–194, [hep-ph/0512090].

[3] T. Golling et al., *Physics at a 100 TeV pp collider: beyond the Standard Model phenomena*, *Submitted to: Phys. Rept.* (2016) [arXiv:1606.00947].

[4] E. Bernreuther, J. Horak, T. Plehn, and A. Butter, *Actual Physics behind Mono-X*, arXiv:1805.11637.

[5] M. Low and L.-T. Wang, *Neutralino dark matter at 14 TeV and 100 TeV*, *JHEP* **08** (2014) 161, [arXiv:1404.0682].

[6] **ATLAS** Collaboration, M. Aaboud et al., *Search for new phenomena in final states with an energetic jet and large missing transverse momentum in pp collisions at $\sqrt{s} = 13$ TeV using the ATLAS detector*, *Phys. Rev.* **D94** (2016), no. 3 032005, [arXiv:1604.07773].

[7] **CMS** Collaboration, A. M. Sirunyan et al., *Search for dark matter produced with an energetic jet or a hadronically decaying W or Z boson at $\sqrt{s} = 13$ TeV*, arXiv:1703.01651.

[8] **ATLAS** Collaboration, T. A. collaboration, *Search for new phenomena in the $Z(\to \ell\ell) + E_{\mathrm{T}}^{\mathrm{miss}}$ final state at $\sqrt{s} = 13$ TeV with the ATLAS detector*, .

[9] **CMS** Collaboration, A. M. Sirunyan et al., *Search for new physics in events with a leptonically decaying Z boson and a large transverse momentum imbalance in proton-proton collisions at $\sqrt{s} = 13$ TeV*, arXiv:1711.00431.

[10] **ATLAS** Collaboration, M. Aaboud et al., *Search for dark matter at $\sqrt{s} = 13$ TeV in final states containing an energetic photon and large missing transverse momentum with the ATLAS detector*, *Eur. Phys. J.* **C77** (2017), no. 6 393, [arXiv:1704.03848].

[11] **CMS** Collaboration, A. M. Sirunyan et al., *Search for new physics in the monophoton final state in proton-proton collisions at $\sqrt{s} = 13$ TeV*, *JHEP* **10** (2017) 073, [arXiv:1706.03794].

[12] S. Gori, S. Jung, and L.-T. Wang, *Cornering electroweakinos at the LHC*, *JHEP* **10** (2013) 191, [arXiv:1307.5952].

[13] C. Han, A. Kobakhidze, N. Liu, A. Saavedra, L. Wu, and J. M. Yang, *Probing Light Higgsinos in Natural SUSY from Monojet Signals at the LHC*, *JHEP* **02** (2014) 049, [arXiv:1310.4274].

[14] P. Schwaller and J. Zurita, *Compressed electroweakino spectra at the LHC*, *JHEP* **03** (2014) 060, [arXiv:1312.7350].

[15] Z. Han, G. D. Kribs, A. Martin, and A. Menon, *Hunting quasidegenerate Higgsinos*, *Phys. Rev.* **D89** (2014), no. 7 075007, [arXiv:1401.1235].

[16] D. Barducci, A. Belyaev, A. K. M. Bharucha, W. Porod, and V. Sanz, *Uncovering Natural Supersymmetry via the interplay between the LHC and Direct Dark Matter Detection*, *JHEP* **07** (2015) 066, [arXiv:1504.02472].

[17] H. Baer, A. Mustafayev, and X. Tata, *Monojets and mono-photons from light higgsino pair production at LHC14*, *Phys. Rev.* **D89** (2014), no. 5 055007, [arXiv:1401.1162].

[18] M. Cirelli, F. Sala, and M. Taoso, *Wino-like Minimal Dark Matter and future colliders*, *JHEP* **10** (2014) 033, [arXiv:1407.7058]. [Erratum: JHEP01,041(2015)].

[19] A. Anandakrishnan, L. M. Carpenter, and S. Raby, *Degenerate gaugino mass region and mono-boson collider signatures*, *Phys. Rev.* **D90** (2014), no. 5 055004, [arXiv:1407.1833].

[20] T. Han, D. L. Rainwater, and D. Zeppenfeld, *Drell-Yan plus missing energy as a signal for extra dimensions*, *Phys. Lett.* **B463** (1999) 93–98, [hep-ph/9905423].

[21] A. Alves and K. Sinha, *Searches for Dark Matter at the LHC: A Multivariate Analysis in the Mono-Z Channel*, Phys. Rev. **D92** (2015), no. 11 115013, [arXiv:1507.08294].

[22] N. F. Bell, J. B. Dent, A. J. Galea, T. D. Jacques, L. M. Krauss, and T. J. Weiler, *Searching for Dark Matter at the LHC with a Mono-Z*, Phys. Rev. **D86** (2012) 096011, [arXiv:1209.0231].

[23] R. Mahbubani, P. Schwaller, and J. Zurita, *Closing the window for compressed Dark Sectors with disappearing charged tracks*, arXiv:1703.05327.

[24] J. Fan and M. Reece, *In Wino Veritas? Indirect Searches Shed Light on Neutralino Dark Matter*, JHEP **10** (2013) 124, [arXiv:1307.4400].

[25] T. Cohen, M. Lisanti, A. Pierce, and T. R. Slatyer, *Wino Dark Matter Under Siege*, JCAP **1310** (2013) 061, [arXiv:1307.4082].

[26] K. Kowalska and E. M. Sessolo, *The discreet charm of higgsino dark matter - a pocket review*, 2018. arXiv:1802.04097.

[27] R. Krall and M. Reece, *Last Electroweak WIMP Standing: Pseudo-Dirac Higgsino Status and Compact Stars as Future Probes*, arXiv:1705.04843.

[28] M. Baryakhtar, J. Bramante, S. W. Li, T. Linden, and N. Raj, *Dark Kinetic Heating of Neutron Stars and An Infrared Window On WIMPs, SIMPs, and Pure Higgsinos*, Phys. Rev. Lett. **119** (2017), no. 13 131801, [arXiv:1704.01577].

[29] M. Gronau, C. N. Leung, and J. L. Rosner, *Extending Limits on Neutral Heavy Leptons*, Phys. Rev. **D29** (1984) 2539.

[30] S. Antusch and O. Fischer, *Testing sterile neutrino extensions of the Standard Model at future lepton colliders*, JHEP **05** (2015) 053, [arXiv:1502.05915].

[31] J. C. Helo, M. Hirsch, and Z. S. Wang, *Heavy neutral fermions at the high-luminosity LHC*, arXiv:1803.02212.

[32] D. Curtin et al., *Exotic decays of the 125 GeV Higgs boson*, Phys. Rev. **D90** (2014), no. 7 075004, [arXiv:1312.4992].

[33] D. Curtin and C. B. Verhaaren, *Discovering Uncolored Naturalness in Exotic Higgs Decays*, JHEP **12** (2015) 072, [arXiv:1506.06141].

[34] R. Mahbubani and L. Senatore, *The Minimal model for dark matter and unification*, Phys. Rev. **D73** (2006) 043510, [hep-ph/0510064].

[35] S. D. Thomas and J. D. Wells, *Phenomenology of Massive Vectorlike Doublet Leptons*, Phys. Rev. Lett. **81** (1998) 34–37, [hep-ph/9804359].

[36] G. F. Giudice and A. Romanino, *Split supersymmetry*, Nucl. Phys. **B699** (2004) 65–89, [hep-ph/0406088]. [Erratum: Nucl. Phys.B706,487(2005)].

[37] J. Alwall, R. Frederix, S. Frixione, V. Hirschi, F. Maltoni, O. Mattelaer, H. S. Shao, T. Stelzer, P. Torrielli, and M. Zaro, *The automated computation of tree-level and next-to-leading order differential cross sections, and their matching to parton shower simulations*, JHEP **07** (2014) 079, [arXiv:1405.0301].

[38] J. Pumplin, D. R. Stump, J. Huston, H. L. Lai, P. M. Nadolsky, and W. K. Tung, *New generation of parton distributions with uncertainties from global QCD analysis*, JHEP **07** (2002) 012, [hep-ph/0201195].

[39] T. Sjostrand, S. Mrenna, and P. Z. Skands, *PYTHIA 6.4 Physics and Manual*, JHEP **05** (2006) 026, [hep-ph/0603175].

[40] **DELPHES 3** Collaboration, J. de Favereau, C. Delaere, P. Demin, A. Giammanco, V. Lemaître, A. Mertens, and M. Selvaggi, *DELPHES 3, A modular framework for fast simulation of a generic collider experiment*, JHEP **02** (2014) 057, [arXiv:1307.6346].

[41] M. Cacciari, G. P. Salam, and G. Soyez, *FastJet User Manual*, Eur. Phys. J. **C72** (2012) 1896, [arXiv:1111.6097].

[42] M. Cacciari, G. P. Salam, and G. Soyez, *The Anti-k(t) jet clustering algorithm*, JHEP **04** (2008) 063, [arXiv:0802.1189].

[43] E. Conte, B. Fuks, and G. Serret, *MadAnalysis 5, A User-Friendly Framework for Collider Phenomenology*, Comput. Phys. Commun. **184** (2013) 222–256, [arXiv:1206.1599].

[44] E. Conte, B. Dumont, B. Fuks, and C. Wymant, *Designing and recasting LHC analyses with MadAnalysis 5*, Eur. Phys. J. **C74** (2014), no. 10 3103, [arXiv:1405.3982].

[45] D. Yang and Q. Li, *Probing the Dark Sector through Mono-Z Boson Leptonic Decays*, arXiv:1711.09845.

[46] **CMS** Collaboration, A. M. Sirunyan et al., *Search for dark matter and unparticles in events with a Z boson and missing transverse momentum in proton-proton collisions at $\sqrt{s} = 13$ TeV*, JHEP **03** (2017) 061, [arXiv:1701.02042]. [Erratum: JHEP09,106(2017)].

[47] **ATLAS** Collaboration, M. Aaboud et al., *Search for an invisibly decaying Higgs boson or dark matter candidates produced in association with a Z boson in pp collisions at $\sqrt{s} = 13$ TeV with the ATLAS detector*, Phys. Lett. **B776** (2018) 318–337, [arXiv:1708.09624].

[48] G. F. Giudice, B. Gripaios, and R. Mahbubani, *Counting dark matter particles in LHC events*, Phys. Rev. **D85** (2012) 075019, [arXiv:1108.1800].

[49] M. Neubert, J. Wang, and C. Zhang, *Higher-Order QCD Predictions for Dark Matter Production in Mono-Z Searches at the LHC*, JHEP **02** (2016) 082, [arXiv:1509.05785].

[50] J. M. Lindert et al., *Precise predictions for V+ jets dark matter backgrounds*, Eur. Phys. J. **C77** (2017), no. 12 829, [arXiv:1705.04664].

[51] B. Mele, P. Nason, and G. Ridolfi, *QCD radiative corrections to Z boson pair production in hadronic collisions*, Nucl. Phys. **B357** (1991) 409–438.

[52] T. Becher and X. Garcia i Tormo, *Addendum: Electroweak Sudakov effects in W, Z and gamma production at large transverse momentum*, Phys. Rev. **D92** (2015), no. 7 073011, [arXiv:1509.01961].

[53] L. Calibbi, A. Mariotti, and P. Tziveloglou, *Singlet-Doublet Model: Dark matter searches and LHC constraints*, JHEP **10** (2015) 116, [arXiv:1505.03867].

[54] **Planck** Collaboration, P. A. R. Ade et al., *Planck 2015 results. XIII. Cosmological parameters*, Astron. Astrophys. **594** (2016) A13, [arXiv:1502.01589].

[55] A. Alloul, N. D. Christensen, C. Degrande, C. Duhr, and B. Fuks, *FeynRules 2.0 - A complete toolbox for tree-level phenomenology*, Comput. Phys. Commun. **185** (2014) 2250–2300, [arXiv:1310.1921].

[56] A. Belyaev, N. D. Christensen, and A. Pukhov, *CalcHEP 3.4 for collider physics within and beyond the Standard Model*, Comput. Phys. Commun. **184** (2013) 1729–1769, [arXiv:1207.6082].

[57] G. Bélanger, F. Boudjema, A. Pukhov, and A. Semenov, *micrOMEGAs4.1: two dark matter candidates*, Comput. Phys. Commun. **192** (2015) 322–329, [arXiv:1407.6129].

[58] **XENON** Collaboration, E. Aprile et al., *Dark Matter Search Results from a One Tonne×Year Exposure of XENON1T*, arXiv:1805.12562.

[59] G. Jungman, M. Kamionkowski, and K. Griest, *Supersymmetric dark matter*, *Phys. Rept.* **267** (1996) 195–373, [`hep-ph/9506380`].

[60] G. Busoni et al., *Recommendations on presenting LHC searches for missing transverse energy signals using simplified s-channel models of dark matter*, [`arXiv:1603.04156`].

[61] M. Hoferichter, J. Ruiz de Elvira, B. Kubis, and U.-G. Meißner, *High-Precision Determination of the Pion-Nucleon σ Term from Roy-Steiner Equations*, *Phys. Rev. Lett.* **115** (2015) 092301, [`arXiv:1506.04142`].

[62] P. Junnarkar and A. Walker-Loud, *Scalar strange content of the nucleon from lattice QCD*, *Phys. Rev.* **D87** (2013) 114510, [`arXiv:1301.1114`].

[63] C. Cheung, L. J. Hall, D. Pinner, and J. T. Ruderman, *Prospects and Blind Spots for Neutralino Dark Matter*, *JHEP* **05** (2013) 100, [`arXiv:1211.4873`].

[64] **XENON** Collaboration, E. Aprile et al., *Physics reach of the XENON1T dark matter experiment*, *JCAP* **1604** (2016), no. 04 027, [`arXiv:1512.07501`].

[65] **LZ** Collaboration, D. S. Akerib et al., *LUX-ZEPLIN (LZ) Conceptual Design Report*, [`arXiv:1509.02910`].

[66] **DARWIN** Collaboration, J. Aalbers et al., *DARWIN: towards the ultimate dark matter detector*, [`arXiv:1606.07001`].

[67] J. Billard, L. Strigari, and E. Figueroa-Feliciano, *Implication of neutrino backgrounds on the reach of next generation dark matter direct detection experiments*, *Phys. Rev.* **D89** (2014), no. 2 023524, [`arXiv:1307.5458`].

[68] R. J. Hill and M. P. Solon, *WIMP-nucleon scattering with heavy WIMP effective theory*, *Phys. Rev. Lett.* **112** (2014) 211602, [`arXiv:1309.4092`].

[69] G. Cowan, K. Cranmer, E. Gross, and O. Vitells, *Asymptotic formulae for likelihood-based tests of new physics*, *Eur. Phys. J.* **C71** (2011) 1554, [`arXiv:1007.1727`]. [Erratum: Eur. Phys. J.C73,2501(2013)].